ONCOIMMUNOLOGY
2021, VOL. 10, NO. 1, e1954761 (11 pages)
https://doi.org/10.1080/2162402X.2021.1954761

Taylor & Francis
Taylor & Francis Group

ORIGINAL RESEARCH

OPEN ACCESS Check for updates

Expression of the immune checkpoint receptors PD-1, LAG3, and TIM3 in the immune context of stage II and III gastric cancer by using single and chromogenic multiplex immunohistochemistry

Yujun Park[a,b], An Na Seo[c], Jiwon Koh[a,d], Soo Kyoung Nam[a,d], Yoonjin Kwak[a,d], Sang-Hoon Ahn[e], Do Joong Park[f], Hyung-Ho Kim[e,f], and Hye Seung Lee[a,d]

[a]Department of Pathology, Seoul National University College of Medicine, Seoul, Republic of Korea; [b]Department of Pathology, Seoul National University Bundang Hospital, Seongnam-si, Republic of Korea; [c]Department of Pathology, School of Medicine, Kyungpook National University, Kyungpook National University Chilgok Hospital, Daegu, Republic of Korea; [d]Department of Pathology, Seoul National University Hospital, Seoul, Republic of Korea; [e]Department of Surgery, Seoul National University Bundang Hospital, Seongnam-si, Republic of Korea; [f]Department of Surgery, Seoul National University College of Medicine, Seoul, Republic of Korea

ABSTRACT

We sought to determine the clinicopathological significance of PD-1, LAG3, and TIM3 in gastric cancer (GC) by examining their expression and immune context. Immunohistochemistry (IHC) for PD-1, TIM3, LAG3, and tumor-infiltrating immune cell (TIIC) markers was performed in 385 stage II/III GCs. Epstein-Barr virus (EBV) and microsatellite stability (MSI) testing were performed for molecular classification. Chromogenic multiplex IHC (mIHC) for PD1, TIM3, LAG3, CD3, CD8, FOXP3, CD68, and cytokeratin was performed in 58 of the total samples. PD-1, LAG3, and TIM3 expression in TIICs was observed in 91 (23.6%), 193 (50.1%), and 257 (66.8%) GCs by single IHC, respectively. The expression was associated with EBV^+ and MSI-H molecular subtypes ($p \le 0.001$). A positive expression of LAG3 in the invasive margin of the tumor was associated with better prognosis in univariate ($p = .020$) and multivariate ($p = .026$) survival analyses. The expression of different immune checkpoint receptors (ICRs) was significantly positively correlated. Dual or triple ICR expression was more frequent in high PD-1 and TIM3 density groups than in low-density groups by mIHC (all $p \le 0.05$). ICRs were mainly expressed in $CD3^+CD8^+$ and $CD3^+CD8^-$ T cells. Fifty-eight GCs were classified into three groups by clustering analysis based on mIHC, and the group with the highest ICR expression in TIICs showed significantly better outcomes in progression-free survival ($p = .020$). In GC, PD-1, LAG3, and TIM3 expression is positively correlated and associated with better prognosis. Our study provides information for the application of effective immune checkpoint inhibitors against GC.

ARTICLE HISTORY
Received 9 April 2021
Revised 30 June 2021
Accepted 8 July 2021

KEYWORDS
gastric cancer; immune checkpoint receptor; immune context; immunohistochemistry

INTRODUCTION

Gastric cancer (GC) is one of the most common cancers worldwide and the third leading cause of cancer-related deaths. GC is more frequent in East Asia than in Western countries, and it is the second most common cancer in South Korea.[1] Since the success of the TOGA trial,[2] trastuzumab has been used in palliative chemotherapy for advanced GC patients, and few targeted therapies, such as ramucirumab, have also been approved for same. Recently, immune checkpoint inhibitors targeting programmed death receptor 1 (PD-1) were proved to be highly effective in some GC patients. Based on the results of the KEYNOTE 059 trial, pembrolizumab was approved by the FDA in 2017 for pre-treated metastatic and programmed death-ligand 1 (PD-L1)-expressing GC patients.[3,4] The PD-1/PD-L1 checkpoint plays an important role in host immune system evasion in various cancers.[5] PD-L1 expression in GC has been reported in previous studies, and it has been observed in the membranes of GC cells and in the cytoplasm with or without membrane expression of various immune cells. In particular, PD-L1 expression is significantly positively correlated with Epstein-Barr virus (EBV)-associated GCs and microsatellite instability-high (MSI-H) GCs,[6] which are characterized by immune cell-rich stroma.

In addition to PD-1, several immune checkpoint receptors (ICRs) control T cell-mediated cytotoxic reactions, including lymphocyte activation gene-3 (LAG3) and T cell immunoglobulin and mucin domain 3 (TIM3). LAG3 is a potential cancer immunotherapeutic target because it regulates T cell activity. It is structurally similar to CD4,[7] binds to MHC class II molecules expressed by antigen-presenting cells or aberrantly by cancer cells, and mediates an intrinsic negative inhibitory signal, resulting in immune tolerance and immune evasion of cancer cells.[8] LAG3 is expressed on activated human T and NK cells.[9] TIM3 is a member of the TIM gene family and plays a role in suppressing T cell responses and inducing peripheral immune tolerance.[10] It is predominantly expressed in tumor-infiltrating lymphocytes (TILs) of various cancers including prostate cancer, renal cell carcinoma, colorectal cancer, and cervical cancer.[11] However, a comprehensive analysis of the expression of these ICRs in GC is lacking, especially regarding the expression status when considering intratumoral heterogeneity and clinicopathologic implications.

CONTACT Hye Seung Lee hye2@snu.ac.kr Department of Pathology, Seoul National University College of Medicine, Seoul, Republic of Korea
Supplemental data for this article can be accessed on the publisher's website

Recently, several targeted and immunotherapeutic agents were approved for palliative therapy in patients with recurrent or metastatic cancer. Based on the successful results of immune checkpoint inhibitors in trials of metastatic melanoma patients, a few new studies have evaluated the immunotherapeutic effects in high-risk resected stage III melanomas.[12] Although PD-1 inhibitors have shown therapeutic potential in various advanced cancers, including GC, the therapeutic response rates are still unsatisfactory, even in patients with PD-L1 expression. To overcome this, recent studies have tried to employ immune checkpoint inhibitors for combination therapy, including combination with other immune checkpoint inhibitors, targeted agents, radiation, and conventional chemotherapeutic agents.[13] Importantly, the intracellular signaling pathway after interaction of PD-1 with PD-L1 is different from the intracellular pathways that are triggered upon binding of LAG3 and TIM3 to their specific ligands.[14] Dual blockade of PD-1 and LAG3 has been suggested to synergistically restore T cell function in cancer.[15] Previous studies have also suggested that PD-1 and TIM3 cooperate in the suppression of T cell responses and that their co-blockade results in greater reinvigoration of effector T cell responses.[16] However, the co-expression status of various ICRs has not been clarified. Therefore, a comprehensive investigation of the immune microenvironment is necessary for managing cancer patients.

Immunotherapeutic agents are not only used for palliative therapy. For example, clinical trials are underway to combine cisplatin and 5-FU, the first-line therapy for patients with advanced GC, for neoadjuvant or adjuvant treatment.[17] In addition, chemotherapy reportedly has an effect on the tumor microenvironment (TME). Chemotherapy activates the immune response to tumors by strengthening the response of cytotoxic T cells, increasing antigenicity to cancer, or inhibiting immunosuppressive pathways.[18,19] However, there are insufficient research results related to the expression pattern of ICRs, such as PD-1, and the co-expression of ICRs in patients with GC who are the targets of radical surgery. Therefore, the need for information on the expression of ICRs in patients with GC undergoing adjuvant chemotherapy after radical surgery or radical surgery after neoadjuvant chemotherapy is increasing.

In this study, we aimed to reveal the clinicopathological implications of the ICRs, PD-1, TIM3, and LAG3 using single immunohistochemistry (IHC), and to analyze their expression based on immune cell context and their co-expression using multiplex immunohistochemistry (mIHC) in stage II and III GCs.

MATERIALS AND METHODS

Patients and samples

A total of 385 patients with stage II or III GC who underwent curative surgical resection at Seoul National University Bundang Hospital (Seongnam-si, Republic of Korea) between 2006 and 2013 were retrospectively enrolled. After radical surgery, the patients were treated with fluoropyrimidine (FP)-based adjuvant chemotherapy. Clinicopathologic features, including overall survival (OS) and progression-free survival (PFS), were obtained from medical records and pathology reports. Tissue microarrays (TMAs) were constructed from formalin-fixed and paraffin-embedded (FFPE) samples. Two separate 2 mm cores were selected from both the center and the invasive margin of the tumor for each case.

Single IHC

All antibodies and staining devices used for single IHC are listed in Supplementary Table 1.

Interpretation of PD-1, TIM3, and LAG3 expression

PD-1, LAG3, and TIM3 expression was observed in the membranes with or without cytoplasm of tumor-infiltrating immune cells (TIICs), and interpreted as the extent (%) of immunostained TIICs. Positive expression was defined as immunostaining ≥ 5% of the immune cells.[20]

Interpretation of PD-L1, E-cadherin, p53, and HER2 expression

PD-L1 expression was evaluated using the combined positive score (CPS) method. The cases were considered PD-L1$^+$ if the CPS was one or more.[20]

For E-cadherin, strong staining on the membrane of tumor cells was defined as positive expression, and if membrane staining was completely lost or abnormal cytoplasmic staining was observed, it was evaluated as altered expression.

For p53 expression in tumor cells, strong nuclear staining in 10% or more of the cells was interpreted as p53 overexpression/positive, and cases with less than 10% positive cells, including those showing scattered positive or patchy positive cells, were considered negative.[21]

HER2 protein expression was assessed based on the staining intensity of tumor cell membranes. The scoring was classified into four categories based on the intensity of membrane staining (0 or 1+, negative; 2+, equivocal; 3+, positive), if 10% or more tumor cells were stained.[22]

Evaluation of immune cell density for CD3, CD4, CD8, Foxp3, CD68, and CD163 expression

All immunostained TMA slides were digitally scanned using an X400 Aperio ScanScope CS instrument (Aperio Technologies, Vista, CA, USA). The cell densities (number of positively stained cells per mm^2) in each core of the TMA slides were determined using an Aperio image analysis system (Leica Biosystems, New Castle, UK).[6]

MSI analysis

DNA extraction and polymerase chain reaction (PCR) of 5 National Cancer Institute (NCI) markers (BAT-26, BAT-25, D5S346, D17S250, and S2S123) were performed in both tumor cells and matched normal samples. PCR products from the FFPE samples were analyzed with an automatic sequencer (ABI 3731 Genetic Analyzer; Applied Biosystems, Foster City, CA, USA) according to a previously described protocol.[23] MSI status was assessed by comparing the allele profiles of two

unstable marker as MSI-high (MSI-H), one unstable marker as MSI-low (MSI-L), and no unstable marker as microsatellite stable (MSS).

EBV in situ hybridization (ISH)

To determine the EBV status of tumor cells, EBV ISH was performed using an INFORM EBV-encoded RNA probe (Ventana Medical Systems, Tucson, AZ, USA). GC samples with cancer cells positive for nuclear EBER were considered EBV-positive.

Molecular classification in GC

We classified the GC samples used in the study into five subgroups (EBV^+, MSI-H, epithelial-mesenchymal transition (EMT)-like, $p53^+$, and $p53^-$) using E-cadherin and p53 IHC, EBV ISH, and MSI status.[23]

mIHC for ICRs and immune cells

We performed mIHC on TMA slides composed of 58 samples selected from the center of the tumor among the total GC samples. All implementations and analysis of mIHC were performed on the SuperBioChips (SuperBioChips Laboratories, Seoul, Korea). All antibodies and reagents used for mIHC are listed in Supplementary Table 2. First, Harris hematoxylin (Merck, Darmstadt, Germany) was used for nuclear staining. After incubation with the primary antibody (Supplementary Table 2) and washing twice with wash buffer (Dako, Carpinteria, CA, USA), the Envision FLEX + mouse linker/rabbit linker (Dako, Carpinteria, CA, USA) was treated with a secondary reagent. For chromogenic reaction and visualization, ImmPact NovaRED (Vector Laboratories, Burlingame, CA, USA) was used. Mayer's hematoxylin (Dako, Carpinteria, CA, USA) was used for nuclear counterstaining, and all stained slides were subjected to full slide scanning using an Aperio AT2 scanner (Leica Biosystems, Newcastle upon Tyne, UK). After scanning, the slides were treated with a stripping buffer (20% sodium dodecyl sulfate, 0.5 M Tris-HCl pH 6.8, β-mercaptoethanol, and distilled water) and then microwaved for antibody stripping. The staining-scanning-stripping process was repeated sequentially for each primary antibody (Supplementary Table 2).

For analysis, each 2 mm core in the TMA was extracted using an image program. CellProfiler (ver. 3.1.8. Broad Institute, Cambridge, MA) was used to adjust the image position so that the TMA core images extracted from each of the stained slide images could be matched in exactly the same two-dimensional positions. Thus, a single cell in the core represented the minimum unit of analysis. Staining information such as staining intensity for all primary antibodies in single cells was provided as a continuous variable. To assess the positive or negative status of all immunostained markers in each single cell, an appropriate cutoff value for staining intensity was determined (Supplementary Table 2). Cytokeratin staining images were used to evaluate each stained cell separately from the intratumoral and stromal areas. The density of positive cells in stained cells was defined as the number of positive cells per mm^2. More detailed information on mIHC procedures has been provided in previous studies.[24]

Statistical analysis

All analyses were performed using R 3.6.1, RStudio 1.2.5033, and SPSS 25.0 (SPSS, Inc., Chicago, IL, USA). For single IHC, Pearson's chi-square test was used to analyze the association among ICRs, molecular classification markers, and clinicopathologic features. In addition, the McNemar test was used to examine intratumor ICR heterogeneity between tumor centers and peripherals. The association between ICRs and immune cell density was determined using the Pearson correlation coefficient. OS was analyzed using the Kaplan–Meier method and log-rank test, and independent prognostic factors were identified by univariate and multivariate Cox regression analyses.

For mIHC, the Wilcoxon rank-sum test was used to identify statistical significance between two groups, and comparison between multiple groups was performed using the Kruskal-Wallis test with Bonferroni correction in the R function wilcox_test() from the package "rstatix" (Alboukadel Kassambara, 2020, rstatix: Pipe-friendly framework for basic statistical tests. R package version 0.4.0; https://cran.r-project.org/web/packages/rstatix/index.html). Box and whisker plots were used to show the median and quartiles. To determine the ideal cutoff values for establishing high and low cell density groups, we used the 'surv_cutpoint()' function from the package "survminer" (Alboukadel Kassambara (2019), survminer: Drawing Survival Curves using 'ggplot2'. R package version 0.4.6; https://cran.r-project.org/web/packages/survminer/index.html) using the maximally selected rank statistic from the 'maxstat' R package.[25] Following this analysis, the 'analyse_multivariate()' function using Cox regression analysis and 'forest plot()' function from the package "survivalAnalysis" (Marcel Wiesweg (2019), survivalAnalysis: High-Level Interface for Survival Analysis and Associated Plots. R package version 0.1.1; https://cran.r-project.org/web/packages/survivalAnalysis/index.html) was used to perform univariate survival analysis for immune cell and immune checkpoint expressing cell and to create forest plots for each parameter. For cluster analysis, first, data standardization and log-2 transformation were performed, and unsupervised hierarchical clustering using an Euclidean distance measure and complete linkage was performed with the 'hclust()' function from the package "stats." OS for clusters was determined using the Kaplan–Meier method and log-rank test. A probability value of less than 0.05 was considered statistically significant.

RESULTS

Clinicopathologic and prognostic significance of ICR expression

Of the 385 stage II and III GCs, 68 cases (17.7%) showed positive PD-1 expression in the center, 69 (17.9%) in the invasive margin, and 91 (23.6%) in the center or invasive margin. LAG3 expression was found in 175 (45.5%), 114 (29.6%), and 193 (50.1%), and TIM3 in 237 (61.6%), 134

(34.8%), and 257 (66.8%) cases in the center, invasive margin, and center or invasive margin, respectively. PD-1 expression was similar between the center and invasive margin (p = 1.0, McNemar test; Supplementary Table 3). However, LAG3 and TIM3 expression levels were significantly higher in the center than in the invasive margin (p < .001 by McNemar test). The rate of agreement, Cohen's κ values, and the correlation coefficient of PD-1 expression between the center and invasive margin were higher than those of LAG3 and TIM3 (Supplementary Table 3). The clinicopathologic features are summarized in Supplementary Table 4. PD-1 expression was associated with old age, expanding growth, and distal location (p < .05), LAG3 expression with expanding growth and distal location (p < .05), and TIM3 expression with infiltrative growth, unlike PD-1 and LAG3 (p < .05). In addition, TIM3-expressing cases showed more diffuse-type in positive expression than in negative expression when compared with PD-1- and LAG3-expressing cases.

Kaplan-Meier survival analysis showed that GC patients with positive expression of PD-1, TIM3, and LAG3 in the center, invasive margin, and center or invasive margin tended to have better OS than those with negative expression (Supplementary Figure 1), but the difference was only statistically significant in cases where LAG3 was expressed in the invasive margin (p = .019) and center or invasive margin (p = .026). The results of the multivariate survival analysis are summarized in Table 1, and confirmed that LAG3 expression is an independent favorable prognostic factor for OS (invasive margin, p = .026; center or invasive margin, p = .026).

Correlation of ICR expression with immune cell density and molecular classification

PD-1 expression was positively correlated with LAG3 (γ = 0.631) and TIM3 (γ = 0.625) expression (Table 2), and these were classified as strong correlations.[26] LAG3 expression was moderately correlated with TIM3 expression (γ = 0.534). In addition, the expression of these three ICRs showed significant positive correlations with the density of various immune cell types, including $CD3^+$, $CD4^+$, $CD8^+$, $CD68^+$, and $CD163^+$ TIICs. Table 3 shows the relationship between ICR expression and the molecular classification of GC. $PD\text{-}1^+$, $LAG3^+$, and $TIM3^+$ rates were significantly higher in EBV^+ and MSI-H GCs than in EMT-type, $p53^+$, and $p53^-$ GCs (p < .001). In particular, EMT-type GCs showed the lowest positive rate of ICR expression, and the $TIM3^+$ rate was the highest among the three markers.

Table 2. Correlation coefficient between immune checkpoint receptors and immune cell density.

Center				Periphery			
	PD-1	LAG3	TIM3		PD-1	LAG3	TIM3
PD-1	1			PD-1	1		
LAG3	.631**	1		LAG3	.590**	1	
TIM3	.534**	.625**	1	TIM3	.422**	.592**	1
PD-L1 (CPS)	.345**	.345**	.443**	PD-L1 (CPS)	.412**	.643**	.630**
PD-L1 (TPS)	.290**	.307**	.385**	PD-L1 (TPS)	.361**	.604**	.559**
PD-L1 (ICP)	.264**	.187**	.262**	PD-L1 (ICP)	.419**	.519**	.560**
CD3	.561**	.423**	.551**	CD3	.503**	.356**	.568**
CD4	.265**	.203**	.207**	CD4	.311**	.177**	.307**
CD8	.551**	.351**	.582**	CD8	.479**	.346**	.580**
CD68	.332**	.405**	.292**	CD68	.400**	.379**	.470**
CD163	.439**	.305**	.331**	CD163	.573**	.565**	.706**
Foxp3	.342**	.219**	.276**	Foxp3	.515**	.340**	.491**

**p value < 0.01; PD-1, Programmed cell death-1; CK, Cytokeratin; TIM-3, T-cell immunoglobulin and mucin domain-3; LAG-3, Lymphocyte activation gene-3, CPS, Combined positive score; TPS. Tumor proportion score; ICP, Immune cells present

Combined expression status of the three ICRs by mIHC

Since the expression of PD-1, TIM3, and LAG3 was positively correlated, we performed chromogenic mIHC in 58 stage II and III GC cases to investigate their dual and triple expression. The density of cells with single PD-1 (red), TIM3 (green), and LAG3 (blue) expression was determined in each case (Supplementary Figure 2). Then, the density of cells with dual and triple expression was evaluated.

Table 1. Multivariable survival analysis by using Cox-regression analysis.

	Univariate analysis			Multivariate analysis (LAG3 periphery)			Multivariate analysis (LAG3 center or periphery)		
Variables	HR	95% CI	P	HR	95% CI	P	HR	95% CI	p value
Age	1.028	1.010– 1.047	0.002	1.024	1.006– 1.042	< 0.010	1.022	1.004– 1.040	0.018
Size	1.131	1.071– 1.193	< 0.001	1.096	1.031– 1.165	0.003	1.094	1.028– 1.164	0.005
Lauren classification (others vs. intestinal*)	1.443	0.914– 2.276	0.115		-			-	
Ming classification (expanding vs. infiltrative*)	0.65	0.346– 1.222	0.181		-			-	
Lymphatic invasion (present vs. absent*)	1.373	0.849– 2.221	0.197		-			-	
Vascular invasion (present vs. absent*)	3.263	2.102– 5.065	< 0.001	2.105	1.326– 3.341	0.002	2.168	1.363– 3.448	0.001
Perineural invasion (present vs. absent*)	2.891	1.634– 5.114	< 0.001	1.746	0.948– 3.215	0.074	1.824	0.992– 3.354	0.053
pTNM (III vs. II*)	3.439	2.091– 5.655	< 0.001	2.165	1.260– 3.720	0.005	2.2	1.280– 3.782	0.004
LAG3 periphery (positive vs. negative*)	0.536	0.316– 0.908	0.020	0.540	0.315– 0.928	0.026		-	
LAG3 center or periphery (positive vs. negative*)	0.643	0.421– 0.980	0.040		-		0.614	0.400– 0.944	0.026

*Reference variable;LAG-3, Lymphocyte activation gene-3

Table 3. Correlation between immune checkpoint receptors and molecular classification.

		PD-1			LAG-3			TIM-3		
Molecular classification	total	N	P	p value	N	P	p value	N	P	p value
EBV-P	25 (6.5%)	6 (2.0%)	19 (20.9%)	< 0.001	1 (0.5%)	24 (12.4%)	< 0.001	1 (0.8%)	24 (9.3%)	< 0.001
MSI-H	36 (9.4%)	16 (5.4%)	20 (22.0%)		7 (3.6%)	29 (15.0%)		4 (3.1%)	32 (12.5%)	
EMT	104 (27.0%)	100 (34.0%)	4 (4.4%)		74 (38.5%)	30 (15.5%)		47 (36.7%)	57 (22.2%)	
p53 IHC-P	70 (18.2%)	54 (18.4%)	16 (17.6%)		29 (15.1%)	41 (21.2%)		26 (20.3%)	44 (17.1%)	
p53 IHC-N	150 (39.0%)	118 (40.1%)	32 (35.2%)		81 (42.2%)	69 (35.8%)		50 (39.1%)	100 (38.9%)	
total	385	294	91		192	193		128	257	

N, negative; P, positive; MSI-H, microsatellite instability-high; EMT, epithelial-mesenchymal transition; IHC, immunohistochemistry

The mean percentage of cells with dual or triple ICR expression was 23.7% among PD-1$^+$ cells, 26.4% among TIM3$^+$ cells, and 32.1% among LAG3$^+$ cells (Figure 1a-c). The proportion of cells with single, dual, and triple expression among PD-1$^+$, TIM3$^+$, and LAG3$^+$ cells varied in each case (Figure 1d-f).

When the GC cases were classified into high and low groups based on the median PD-1$^+$ and TIM3$^+$ cell densities, the frequency of dual or triple expressing cells was significantly higher in the high-density group (PD-1, 30.6 ± 23.2%; TIM3, 33.8 ± 20.8%) than in the low-density group (PD-1, 16.8 ± 11.1%; TIM3, 19.1 ± 16.1%) (PD-1, p = .023; TIM3, p < .001; Figure 1g and 1h). There was no significant difference in dual or triple expression frequency among LAG3$^+$ cells (p = .130; Figure 1i).

Comprehensive ICR expression analysis based on immune cell context

ICRs were mainly expressed in CD3$^+$/CD8$^+$ and CD3$^+$/CD8$^-$ T cells, and minorly expressed in CD3$^+$/Foxp3$^+$ T cells and CD68$^+$ macrophages (Figure 2a). PD-1 expression was significantly higher in CD3$^+$/CD8$^+$ and CD3$^+$/CD8$^-$ T cells than in CD3$^+$/Foxp3$^+$ T cells and CD68$^+$ macrophages, but TIM3 expression did not significantly differ in CD68$^+$ macrophages when compared with that in CD3$^+$/CD8$^+$ and CD3$^+$/CD8$^-$ T cells (Kruskal–Wallis, PD-1, p <.001; TIM3, p = .010; Figure 2b). LAG3 expression was significantly higher in CD3$^+$/CD8$^+$ T cells than in CD68$^+$ macrophages but did not significantly differ when compared with that in CD3$^+$/CD8$^-$ and CD3$^+$/Foxp3$^+$ T cells (Kruskal–Wallis, LAG3, p = .008;

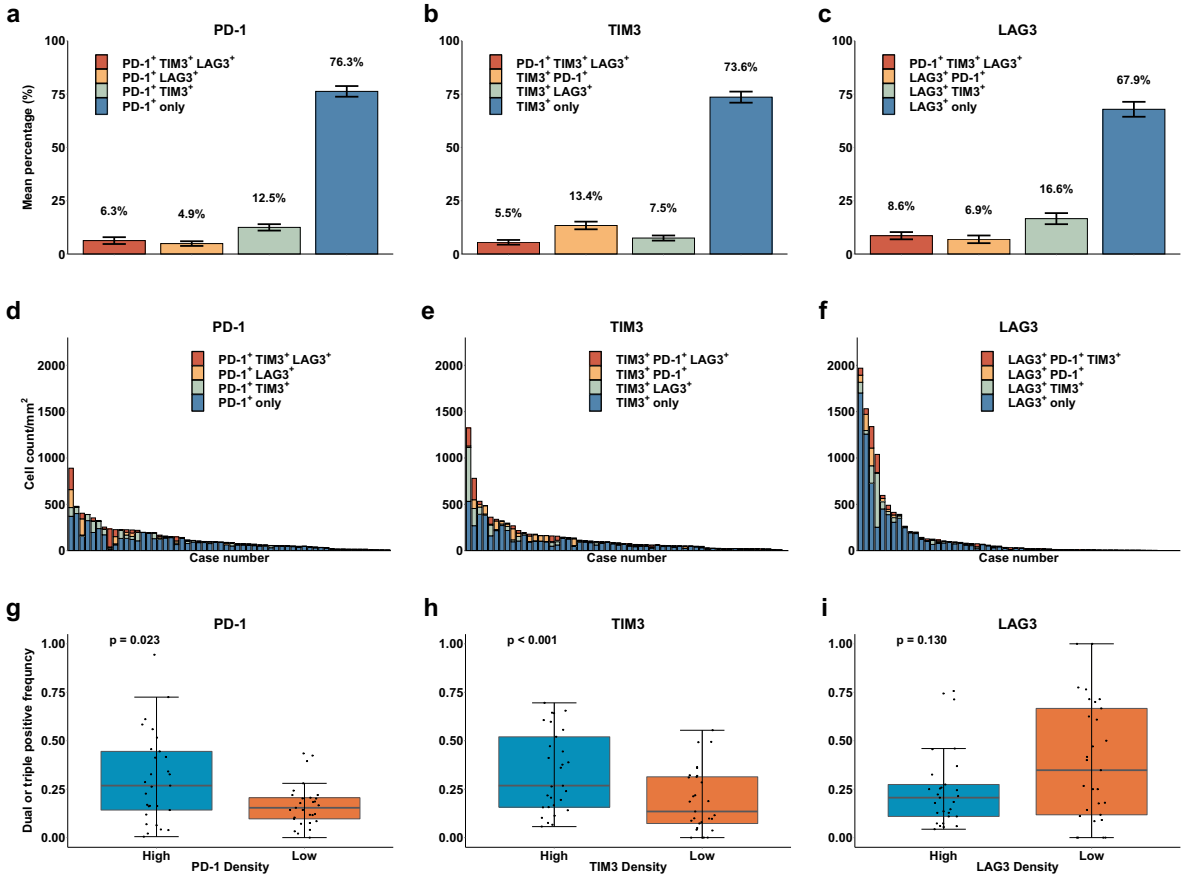

Figure 1. Combined expression of immune checkpoint receptors. Mean percentage of cells expressing single or multiple immune checkpoint receptors (ICRs): programmed death receptor 1 (PD-1) (a), T cell immunoglobulin and mucin domain 3 (TIM3) (b), and lymphocyte activation gene-3 (LAG3) (c). The proportion of cells with single, dual, and triple ICR expression varied in each case: PD-1 (d), TIM3 (e), and LAG3 (f). The frequency of double or triple ICR expression when the samples were divided into high/low density groups based on the median: PD-1 (g), TIM3 (h), and LAG3 (i).

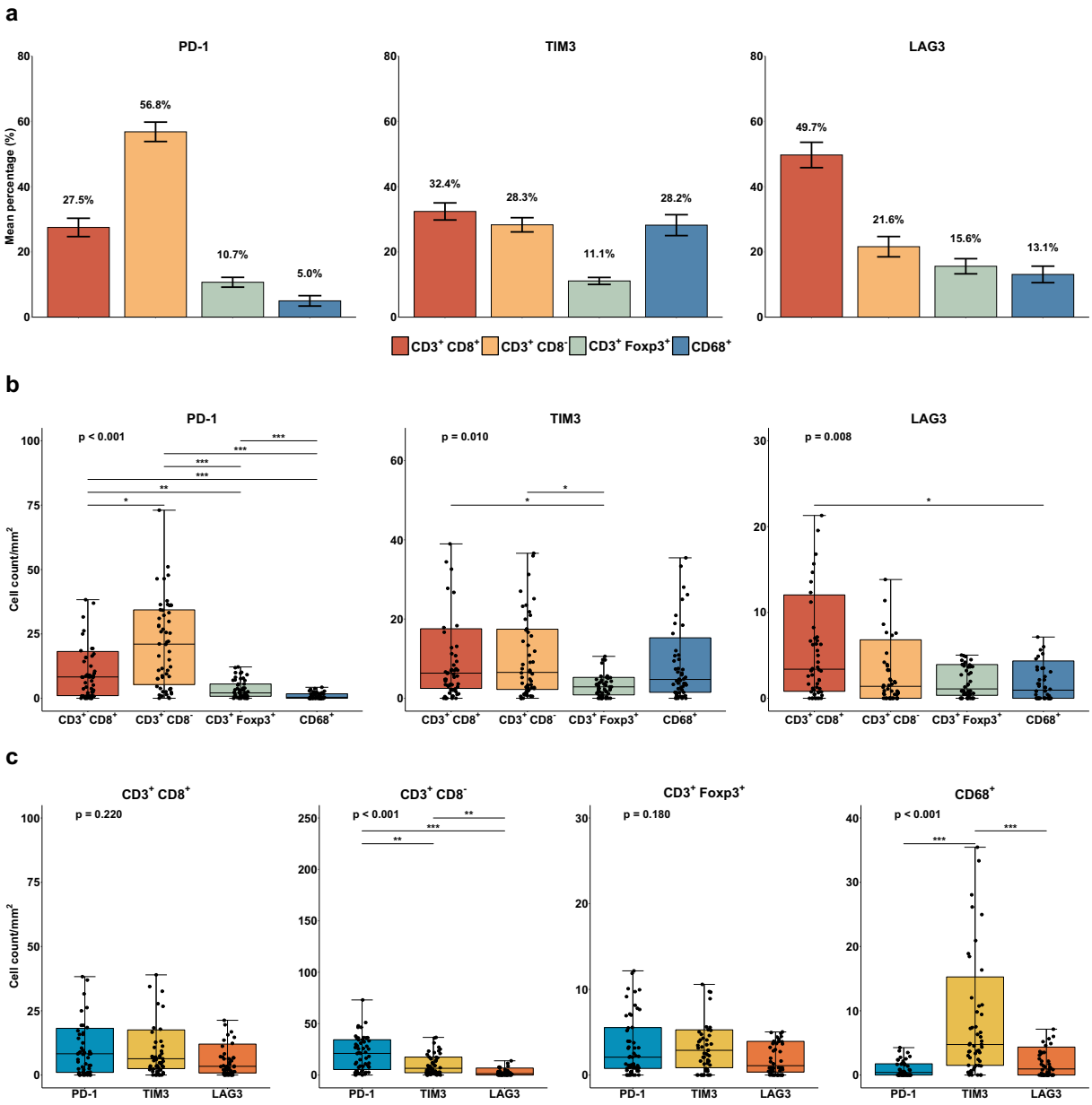

Figure 2. Immune checkpoint receptor expression based on immune context. Mean percentage of immune cell types expressing each immune checkpoint receptor (ICR): programmed death receptor 1 (PD-1), T cell immunoglobulin and mucin domain 3 (TIM3), and lymphocyte activation gene-3 (LAG3) (a). Comparison of the density of each immune cell type expressing each ICR (b). Comparison of the density of ICRs expressed by each immune cell type (c).

Figure 2b). When comparing ICR expression by each immune cell type, PD-1 expression was the highest in $CD3^+/CD8^-$ T cells, while TIM3 expression was the highest in $CD68^+$ macrophages (Kruskal–Wallis, all $p < .001$, Figure 2c). There were no significant differences in expression among the three ICRs in $CD3^+/CD8^+$ and $CD3^+/Foxp3^+$ T cells (Kruskal–Wallis, all $p > .05$, Figure 2c).

In the remaining immune cells, except $CD3^+/CD8^-$ T cells, the mean proportion of double- or triple-expressing immune cells including TIM3 was higher than that without TIM3 expression. (Supplementary Figure 3a). The cell density in the presence of the expression of two or more ICRs was higher in $CD3^+/CD8^+$ T cells than in $CD68^+$ macrophages (Kruskal–Wallis, all $p < .001$, Supplementary Figure 3b.

Regarding the distribution between the intratumoral and stromal areas, only $CD3^+/Foxp3^+$ T cells were more distributed in the intratumoral area than in the stromal area regardless of any ICRs expression ($p < .001$, Figure 3a). $CD3^+/CD8^+$ and $CD3^+/Foxp3^+$ T cells expressing any of the three ICRs were significantly more distributed in the intratumoral area than in the stromal area ($CD3^+/CD8^+/PD\text{-}1^+$, $p < .05$; $CD3^+/CD8^+/LAG3^+$, $p < .001$; $CD3^+/CD8^+$ and $CD3^+/FoxP3^+$ T cells expressing any ICRs, all $p < .01$, Figure 3b).

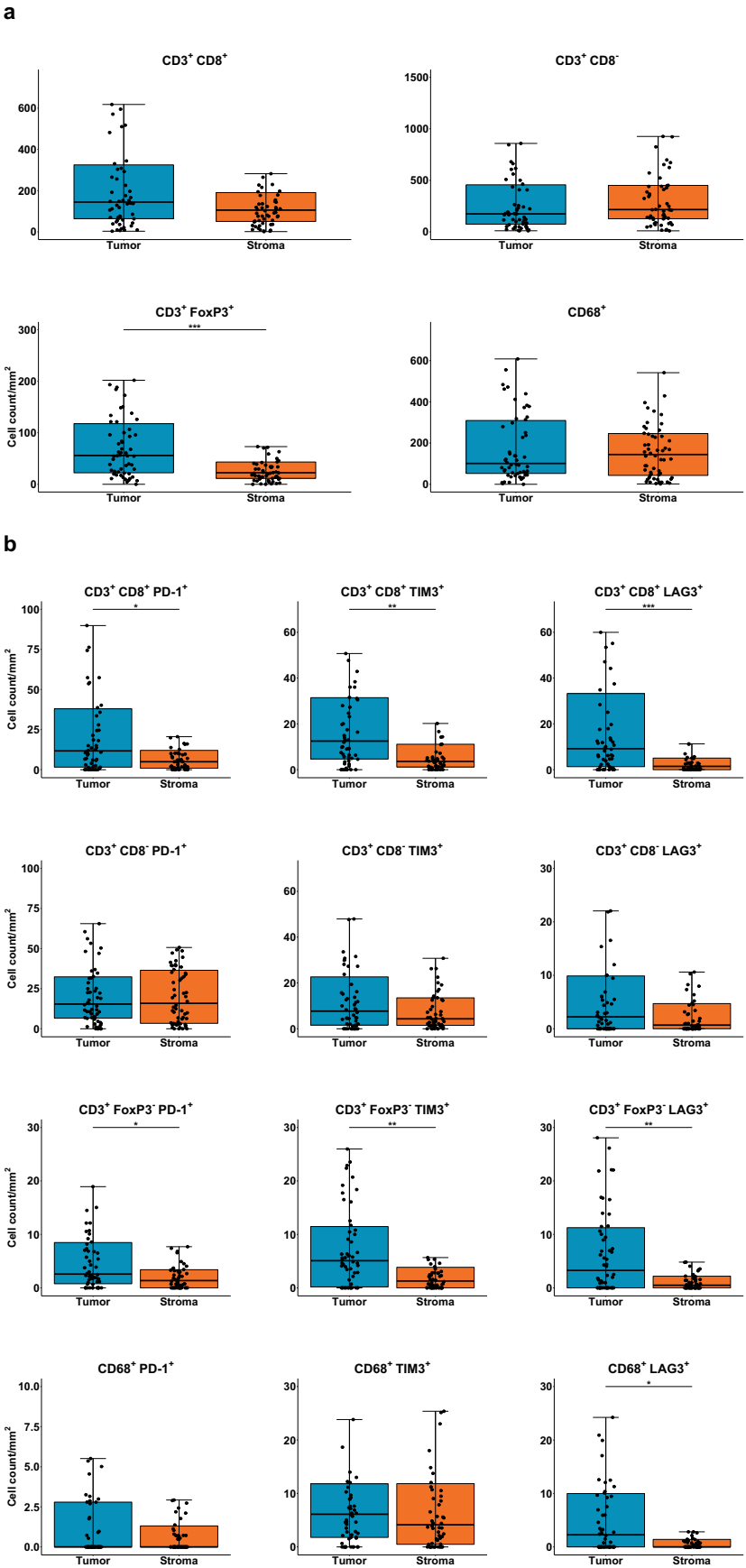

Figure 3. Differences in immune checkpoint receptor expression between tumors and stroma. Comparison of immune cell types between tumor and stromal areas (a). Comparison of immune cell types expressing immune checkpoint receptors between tumor and stromal areas (b).

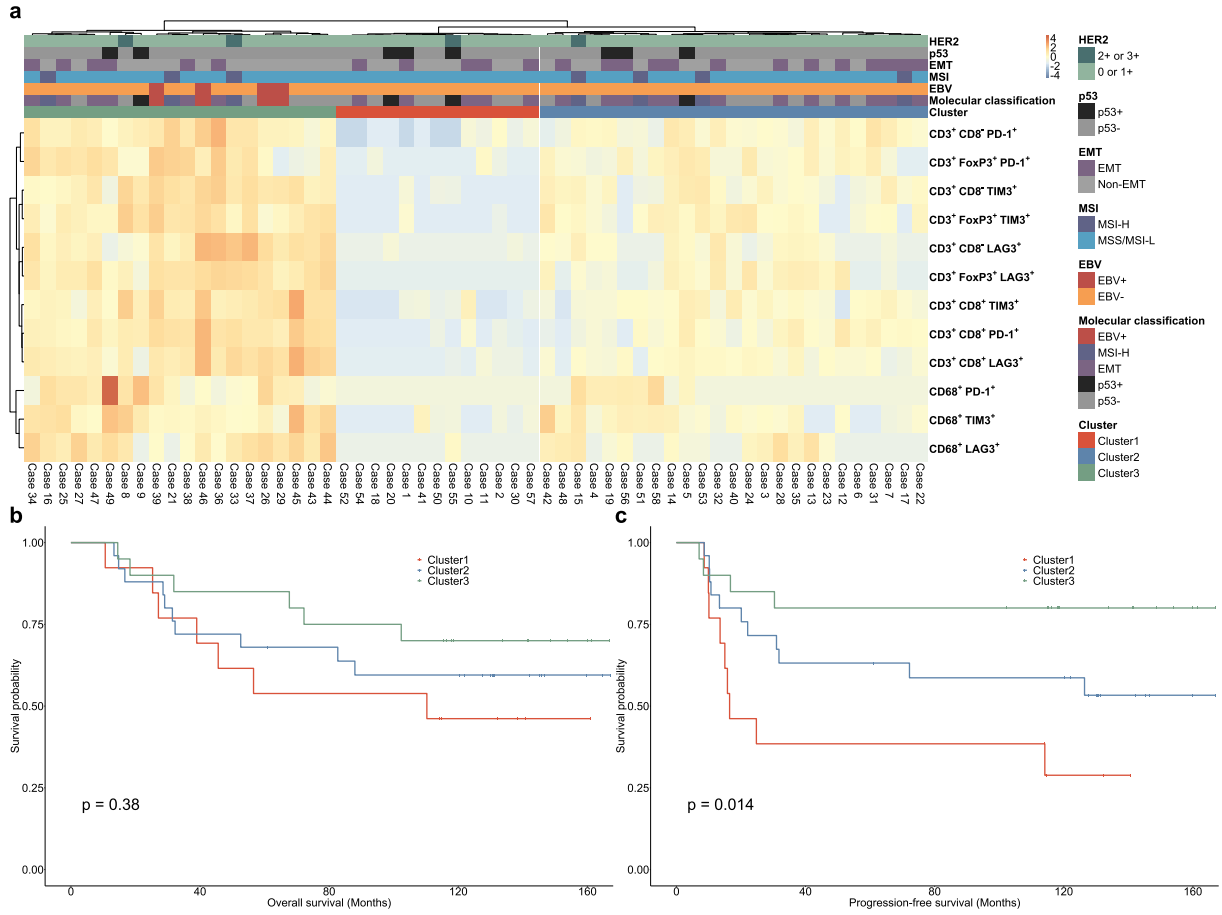

Figure 4. Association between tumor infiltrating immune cell (TIIC) context and the expression of three immune checkpoint receptors (ICRs). Three cluster were identified by unsupervised hierarchical cluster analysis (a). Kaplan Meier survival analysis of the overall survival (OS) (b) and progression-free survival (PFS) (c) in each cluster.

Prognostic analysis of TIIC context and ICR expression by mIHC

The results of univariate Cox analysis showed that a positive expression of PD-1 and TIM3 was significantly positively associated with better OS (both $p < .01$, Supplementary Figure 4a) and PFS (both $p < .001$, Supplementary Figure 4b), unlike in the single IHC. A positive expression of LAG3 was statistically significant only for better PFS ($p = .006$; Supplementary Figure 4b). High numbers of $CD3^+/CD8^+$ and $CD3^+/CD8^-$ T cells among TIICs were associated with better OS (all $p < .05$, Supplementary Fig. S4A) and PFS (all $p < .01$, Supplementary Figure 4b). When not considering ICR expression, high $CD3^+/Foxp3^+$ T cells showed no statistical significance in either better OS ($p = .269$, Supplementary Figure 4a) or PFS ($p = .085$, Supplementary Figure 4b), but high $CD3^+/Foxp3^+$ cells with TIM3 expression showed statistically significant improvements in OS ($p = .012$, Supplementary Figure 4c) and PFS ($p < .001$, Supplementary Figure 4d).

$PD\text{-}1^+/TIM3^+$ and $TIM3^+/LAG3^+$ dual expression showed better OS ($p < .05$, Supplementary Fig. 5A) and PFS ($p < .001$, Supplementary Fig. 5B), but $PD\text{-}1^+/LAG3^+$ showed better results only for PFS ($p = .043$, Supplementary Fig. 5B).

Cluster analysis of TIIC context with ICR expression

Using the TIIC context associated with the expression of the three ICRs, three clusters were identified by unsupervised hierarchical cluster analysis (Figure 4a). The three clusters could be divided into high, medium, and low clusters according to the degree of immune cell density. Most EBV molecular types were located in the high cluster, but the MSI, EMT, $p53^+$, and $p53^-$ types did not differ by cluster. The difference in OS among the three groups was not statistically significant ($p = .38$, Figure 4b), but regarding PFS, the clusters with many ICR-expressing immune cells showed significantly better prognosis ($p = .014$, Figure 4c).

DISCUSSION

In this study, we examined the expression level and tumor heterogeneity of PD-1, TIM3, and LAG3, which are ICRs currently targeted for combination therapy clinical trials, using single IHC. Through chromogenic mIHC, we first examined the interactions between ICRs, then analyzed the correlation between immune cell contexts and ICRs, and finally found the possibility of combination therapy.

TILs including $CD8^+$ T cells can infiltrate tumors and suppress their growth, but ICR expression establishes an immunosuppressive TME.[27] These ICRs can be simultaneously expressed, and it has been reported that when a high level of PD-1 is observed, TIM3 and LAG3 are expressed concurrently.[28,29] It has also been reported that there may be a compensatory mechanism such as TIM3 and LAG3 upregulation in $CD8^+$ T cells after receiving anti-PD-1/PD-L1 therapy.[30] Here, we observed that the expression of ICRs was positively correlated by single IHC and that dual or triple ICR expression occurred frequently in cases with high PD-1 and TIM3 expression by mIHC. These results suggest that a strategy targeting multiple checkpoints simultaneously, rather than a single inhibitory receptor, may be preferable.

We found that the distribution of $CD3^+/CD8^+$ T cells, $CD3^+/CD8^-$ T cells, and $CD68^+$ macrophages did not differ between intratumor and stromal areas when any ICRs expression was not considered. Interestingly, ICR-expressing $CD3^+/CD8^+$ T cells were more distributed in the intratumor area. In hepatocellular carcinoma, more $CD8^+$ T cells expressing high levels of PD-1 were observed in the tumor area than in the peri-tumor area, and this was associated with tissue resident memory T cells (TRMs).[31] TRMs are located close to the tumor and are associated with enhanced cytotoxicity.[32] These TRMs express more checkpoint inhibitors than peripheral memory T cells in the lung[33] and breast.[34] In GC, the relationship between TRMs and the clustering of immunoreceptor-expressing T cells around the tumor has not been examined, and therefore, further studies are required.

In previous studies, PD-1 expression was found to be associated with EBV^+ and MSI-H GC.[35] Here, it was found that not only PD-1, but also LAG3 and TIM3 were associated with the EBV^+ and MSI-H groups. Interestingly, unlike PD-1 and LAG3, TIM3 was more expressed in EMT-type GC and diffuse-type GC than PD-1 and LAG3. Further, overexpression of TIM3 was shown to enhance the metastatic capacity of hepatocellular carcinoma cells by promoting EMT.[36] In a recent study, it was found that TIM3 is highly expressed in peritoneal metastatic samples of GC, and the response to chemotherapy was poor.[37,38] The mechanism whereby TIM3 expression induces EMT in GC has not been clearly elucidated. Therefore, further research is needed to find an immunotheutic target for EMT-type GCs that do not respond well to chemotherapy.

We performed single and multiplex IHC for immune cell markers and ICRs, followed by survival analysis. As a result, a better prognosis was observed in cases in which LAG3 was expressed at the invasive margin of the tumor and in cases with higher numbers of tumor-infiltrating cells expressing PD-1 and TIM3. In addition, the expression of ICRs in $CD3^+/CD8^+$, $CD3^+/CD8^-$ and $CD8^-/Foxp3^+$ T cells, and $CD68^+$ macrophages was associated with a better prognosis. The prognostic implications of ICRs remain controversial. Recent studies have revealed that there was a difference in the association between the expression of ICR and prognosis depending on the type of cancer. In breast cancer, PD-1, TIM3, and LAG3 expression has been reported to improve survival,[39–42] whereas TIM3 expression in ovarian cancer[39,43] and PD-1 and TIM3 expression in lung cancer[39,44] are associated with poor prognosis. In GC, PD-1 expression has been associated with poor prognosis,[45] but also with better survival.[46] A higher $LAG3^+CD4^+/CD4^+$ T cell and $LAG3^+CD8^+/CD8^+$ T cell expression ratio is associated with a better prognosis in advanced GC,[47] whereas a higher $TIM3^+CD4^+/CD4^+$ T cell and $TIM3^+CD8^+/CD8^+$ T cell expression ratio is associated with a poor prognosis.[48] PD-1, LAG3, and TIM3 are associated with exhausted immune cells and negative regulation of immune response.[27] However, in cancer types with good prognosis despite high expression of ICRs, high expression reflects an increased activated immune response.[39] LAG3 is expressed in activated $CD4^+/CD8^+$ T cells and regulatory T cells,[49] and it has been reported that induction of LAG3 expression on the cell surface is the first step required for T cell activity.[50] In addition, the ability of TIM3 to induce immune response activity was recently confirmed.[51] We investigated the correlation between the expression of ICRs and the density of various immune cell types in GC. The results also confirmed a significant positive correlation between ICRs and TIICs.

Co-expression of ICRs has been associated with poor prognosis in renal cell carcinoma,[52] ovarian cancer,[43] and hepatocellular carcinoma,[31] but no studies have been reported so far in GC. Here, by implementing mIHC technique in a large cohort of GC, we were able to assess the co-expression status of PD-1, TIM3, or LAG3, and proved a significant association toward better prognosis. As mentioned above, the effect of ICR expression on prognosis differs among cancer types. However, the research methods employed in the studies also differed, which may explain the observed differences. In addition, our cohort size used to examine co-expression by mIHC was small. Therefore, further research using a larger cohort of GCs is needed.

Our study has some limitations that are worth mentioning. This was a retrospective study and mIHC was performed in a small cohort. However, we were able to limit confounding factors on prognostic analysis using a relatively homogeneous cohort consisting of patients with stage II and III GC who received curative surgical resection followed by fluoropyrimidine-based adjuvant chemotherapy.

In summary, through single IHC, we found that the expression of PD-1, LAG3, and TIM3 was positively correlated, and using mIHC, we demonstrated that dual or triple expression of ICRs is more common in cases with high ICRs' expression by single IHC. ICRs were mainly expressed in $CD3^+/CD8^+$ and $CD3^+/CD8^-$ T cells, and were found to be more densely distributed in the intratumoral area than in the stromal area. Moreover, ICRs were found to be associated with a better prognosis, and clusters with a large number of ICR-expressing immune cells had a better prognosis. In conclusion, our study provides key information for the application of multiple immune checkpoint inhibitors that can be used in combination therapy to treat GC patients.

Disclosure Statement

The authors report no conflict of interest.

Funding

This work was supported by the National Research Foundation of Korea (NRF) grant funded by the Korea government (Ministry of Science and ICT) (No. 2019R1A2C1086180).

ORCID

Hye Seung Lee http://orcid.org/0000-0002-1667-7986

Ethics approval

This study was approved by the Institutional Review Board (IRB) of Seoul National University Bundang Hospital (IRB number: B-1606/349-308). Written patient consent was obtained, and the consent process was waived by the IRB under the condition of anonymization and no additional participant intervention.

References

1. Jung KW, Won YJ, Kong HJ. Cancer statistics in Korea: incidence, mortality, survival, and prevalence in 2015. Cancer Res Treat. 2018;50(2):303–316. doi:10.4143/crt.2018.143.
2. Bang YJ, Van Cutsem E, Feyereislova A. Trastuzumab in combination with chemotherapy versus chemotherapy alone for treatment of HER2-positive advanced gastric or gastro-oesophageal junction cancer (ToGA): a phase 3, open-label, randomised controlled trial. Lancet. 2010;376(9742):687–697. doi:10.1016/S0140-6736(10)61121-X.
3. Fuchs CS, Doi T, RW J. Safety and efficacy of pembrolizumab monotherapy in patients with previously treated advanced gastric and gastroesophageal junction cancer: phase 2 clinical KEYNOTE-059 trial. JAMA Oncol. 2018;4(5):e180013. doi:10.1001/jamaoncol.2018.0013.
4. Fashoyin-Aje L, Donoghue M, Chen H. FDA approval summary: pembrolizumab for recurrent locally advanced or metastatic gastric or gastroesophageal junction adenocarcinoma expressing PD-L1. Oncologist. 2019;24:103–109. doi:10.1634/theoncologist.2018-0221.
5. Azuma T, Yao S, Zhu G. B7-H1 is a ubiquitous antiapoptotic receptor on cancer cells. Blood. 2008;111(7):3635–3643. doi:10.1182/blood-2007-11-123141.
6. Koh J, Ock CY, Kim JW. Clinicopathologic implications of immune classification by PD-L1 expression and CD8-positive tumor-infiltrating lymphocytes in stage II and III gastric cancer patients. Oncotarget. 2017;8(16):26356–26367. doi:10.18632/oncotarget.15465.
7. Wang JH, Meijers R, Xiong Y. Crystal structure of the human CD4 N-terminal two-domain fragment complexed to a class II MHC molecule. Proc Natl Acad Sci U S A. 2001;98(19):10799–10804. doi:10.1073/pnas.191124098.
8. Andrews LP, Marciscano AE, Drake CG. LAG3 (CD223) as a cancer immunotherapy target. Immunol Rev. 2017;276(1):80–96. doi:10.1111/imr.12519.
9. Pardoll DM. The blockade of immune checkpoints in cancer immunotherapy. Nat Rev Cancer. 2012;12(4):252–264. doi:10.1038/nrc3239.
10. Du W, Yang M, Turner A. TIM-3 as a target for cancer immunotherapy and mechanisms of action. Int J Mol Sci. 2017;18(3):645. doi: 10.3390/ijms18030645
11. Das M, Zhu C, Kuchroo VK. Tim-3 and its role in regulating anti-tumor immunity. Immunol Rev. 2017;276(1):97–111. doi:10.1111/imr.12520.
12. Grossmann KF, Othus M, Tarhini AA. SWOG S1404: a phase III randomized trial comparing standard of care adjuvant therapy to pembrolizumab in patients with high risk resected melanoma. J Clin Oncol. 2016;34(suppl):e21032. doi:10.1200/JCO.2016.34.15_suppl.e21032.
13. Malhotra J, Jabbour SK, Aisner J. Current state of immunotherapy for non-small cell lung cancer. Transl Lung Cancer Res. 2017;6(2):196–211. doi:10.21037/tlcr.2017.03.01.
14. Li J, Ni L, Dong C. Immune checkpoint receptors in cancer: redundant by design?. Curr Opin Immunol. 2017;45:37–42. doi:10.1016/j.coi.2017.01.001.
15. Woo SR, Turnis ME, Goldberg MV. Immune inhibitory molecules LAG-3 and PD-1 synergistically regulate T-cell function to promote tumoral immune escape. Cancer Res. 2012;72(4):917–927. doi:10.1158/0008-5472.CAN-11-1620.
16. Fourcade J, Sun Z, Benallaoua M. Upregulation of tim-3 and PD-1 expression is associated with tumor antigen-specific CD8+ T cell dysfunction in melanoma patients. J Exp Med. 2010;207(10):2175–2186. doi:10.1084/jem.20100637.
17. Bang YJ, Van Cutsem E, Fuchs CS. KEYNOTE-585: phase III study of perioperative chemotherapy with or without pembrolizumab for gastric cancer. Future Oncol. 2019;15(9):943–952. doi:10.2217/fon-2018-0581.
18. Galluzzi L, Buque A, Kepp O. Immunological effects of conventional chemotherapy and targeted anticancer agents. Cancer Cell. 2015;28(6):690–714. doi:10.1016/j.ccell.2015.10.012.
19. Zitvogel L, Galluzzi L, Smyth MJ. Mechanism of action of conventional and targeted anticancer therapies: reinstating immunosurveillance. Immunity. 2013;39(1):74–88. doi:10.1016/j.immuni.2013.06.014.
20. Park Y, Koh J, Na HY. PD-L1 testing in gastric cancer by the combined positive score of the 22C3 pharmDx and SP263 assay with clinically relevant cut-offs. Cancer Res Treat. 2020;(3). doi:10.4143/crt.2019.718.
21. Chang MS, Lee JH, Kim JP. Microsatellite instability and epstein-barr virus infection in gastric remnant cancers. Pathol Int. 2000;50(6):486–492. doi:10.1046/j.1440-1827.2000.01072.x.
22. Seo AN, Kwak Y, Kim DW. HER2 status in colorectal cancer: its clinical significance and the relationship between HER2 gene amplification and expression. PLoS One. 2014;9(5):e98528. doi:10.1371/journal.pone.0098528.
23. Koh J, Lee KW, Nam SK. Development and validation of an easy-to-implement, practical algorithm for the identification of molecular subtypes of gastric cancer: prognostic and therapeutic implications. Oncologist. 2019;24(12):e1321–e30. doi:10.1634/theoncologist.2019-0058.
24. Koh J, Kwak Y, Kim J. High-throughput multiplex immunohistochemical imaging of the tumor and its microenvironment. Cancer Res Treat. 2020;52(1):98–108. doi:10.4143/crt.2019.195.
25. Bester AC, Lee JD, Chavez A. An integrated genome-wide CRISPRa approach to functionalize lncRNAs in drug resistance. Cell. 2018;173(649–64):e20. doi:10.1016/j.cell.2018.03.052.
26. Evans JD. Straightforward Statistics for the Behavioral Sciences. Pacific Grove (CA): Brooks/Cole Publishing; 1996.
27. Anderson AC, Joller N, Kuchroo VK. Lag-3, tim-3, and TIGIT: co-inhibitory receptors with specialized functions in immune regulation. Immunity. 2016;44(5):989–1004. doi:10.1016/j.immuni.2016.05.001.
28. Thommen DS, Schreiner J, Müller P. Progression of lung cancer is associated with increased dysfunction of T cells defined by coexpression of multiple inhibitory receptors. Cancer Immunol Res. 2015;3(12):1344–1355. doi:10.1158/2326-6066.CIR-15-0097.
29. Thommen DS, Koelzer VH, Herzig P. A transcriptionally and functionally distinct PD-1(+) CD8(+) T cell pool with predictive potential in non-small-cell lung cancer treated with PD-1 blockade. Nat Med. 2018;24:994–1004.
30. Bialkowski L, Van Der Jeught K, Bevers S. Immune checkpoint blockade combined with IL-6 and TGF-beta inhibition improves the therapeutic outcome of mRNA-based immunotherapy. Int J Cancer. 2018;143(3):686–698. doi:10.1002/ijc.31331.
31. Ma J, Zheng B, Goswami S. PD1(Hi) CD8(+) T cells correlate with exhausted signature and poor clinical outcome in hepatocellular carcinoma. J Immunother Cancer. 2019;7(1):331. doi:10.1186/s40425-019-0814-7.

32. Mueller SN, Mackay LK. Tissue-resident memory T cells: local specialists in immune defence. Nat Rev Immunol. 2016;16(2):79–89. doi:10.1038/nri.2015.3.
33. Ganesan AP, Clarke J, Wood O. Tissue-resident memory features are linked to the magnitude of cytotoxic T cell responses in human lung cancer. Nat Immunol. 2017;18(8):940–950. doi:10.1038/ni.3775.
34. Savas P, Virassamy B, Ye C. Single-cell profiling of breast cancer T cells reveals a tissue-resident memory subset associated with improved prognosis. Nat Med. 2018;24(7):986–993. doi:10.1038/s41591-018-0078-7.
35. De Rosa S, Sahnane N, Tibiletti MG. EBV(+) and MSI gastric cancers harbor high PD-L1/PD-1 expression and high CD8(+) intratumoral lymphocytes. Cancers (Basel). 2018;10(4):102. doi:10.3390/cancers10040102
36. Lin H, Yang B, Teng M. T-cell immunoglobulin mucin-3 as a potential inducer of the epithelial-mesenchymal transition in hepatocellular carcinoma. Oncol Lett. 2017;14:5899–5905.
37. Wang R, Song S, Harada K. Multiplex profiling of peritoneal metastases from gastric adenocarcinoma identified novel targets and molecular subtypes that predict treatment response. Gut. 2020;69(1):18–31. doi:10.1136/gutjnl-2018-318070.
38. Huang L, Wu RL, Xu AM. Epithelial-mesenchymal transition in gastric cancer. Am J Transl Res. 2015;7:2141–2158.
39. Tu L, Guan R, Yang H. Assessment of the expression of the immune checkpoint molecules PD-1, CTLA4, TIM-3 and LAG-3 across different cancers in relation to treatment response, tumor-infiltrating immune cells and survival. Int J Cancer. 2020;147(2):423–439. doi:10.1002/ijc.32785.
40. Byun KD, Hwang HJ, Park KJ. T-cell immunoglobulin mucin 3 expression on tumor infiltrating lymphocytes as a positive prognosticator in triple-negative breast cancer. J Breast Cancer. 2018;21(4):406–414. doi:10.4048/jbc.2018.21.e61.
41. Guo L, Cao C, Goswami S. Tumoral PD-1hiCD8+ T cells are partially exhausted and predict favorable outcome in triple-negative breast cancer. Clin Sci (Lond). 2020;134(7):711–726. doi:10.1042/CS20191261.
42. Burugu S, Gao D, Leung S. LAG-3+ tumor infiltrating lymphocytes in breast cancer: clinical correlates and association with PD-1/PD-L1+ tumors. Ann Oncol. 2017;28(12):2977–2984. doi:10.1093/annonc/mdx557.
43. Fucikova J, Rakova J, Hensler M. TIM-3 dictates functional orientation of the immune infiltrate in ovarian cancer. Clin Cancer Res. 2019;25(15):4820–4831. doi:10.1158/1078-0432.CCR-18-4175.
44. Zhuang X, Zhang X, Xia X. Ectopic expression of TIM-3 in lung cancers: a potential independent prognostic factor for patients with NSCLC. Am J Clin Pathol. 2012;137(6):978–985. doi:10.1309/AJCP9Q6OVLVSHTMY.
45. Eto S, Yoshikawa K, Nishi M. Programmed cell death protein 1 expression is an independent prognostic factor in gastric cancer after curative resection. Gastric Cancer. 2016;19(2):466–471. doi:10.1007/s10120-015-0519-7.
46. Wu Y, Cao D, Qu L. PD-1 and PD-L1 co-expression predicts favorable prognosis in gastric cancer. Oncotarget. 2017;8(38):64066–64082. doi:10.18632/oncotarget.19318.
47. Ohmura H, Yamaguchi K, Hanamura F. OX40 and LAG3 are associated with better prognosis in advanced gastric cancer patients treated with anti-programmed death-1 antibody. Br J Cancer. 2020;122(10):1507–1517. doi:10.1038/s41416-020-0810-1.
48. Cheng G, Li M, Wu J. Expression of tim-3 in gastric cancer tissue and its relationship with prognosis. Int J Clin Exp Pathol. 2015;8:9452–9457.
49. Bae J, Lee SJ, Park CG. Trafficking of LAG-3 to the surface on activated T cells via its cytoplasmic domain and protein kinase C signaling. J Immunol. 2014;193(6):3101–3112. doi:10.4049/jimmunol.1401025.
50. Long L, Zhang X, Chen F. The promising immune checkpoint LAG-3: from tumor microenvironment to cancer immunotherapy. Genes Cancer. 2018;9(5–6):176–189. doi:10.18632/genesandcancer.180.
51. Ocana-Guzman R, Torre-Bouscoulet L, Sada-Ovalle I. TIM-3 regulates distinct functions in macrophages. Front Immunol. 2016;7:229. doi:10.3389/fimmu.2016.00229.
52. Granier C, Dariane C, Combe P. Tim-3 expression on tumor-infiltrating PD-1(+)CD8(+) T cells correlates with poor clinical outcome in renal cell carcinoma. Cancer Res. 2017;77:1075–1082. doi:10.1158/0008-5472.CAN-16-0274.